Jawad Naeem, Adnan Mazari, Funda Buyuk Mazari, Zdenek Kus, Jakub Weiner
Technical University of Liberec, Studentská 1402/2, 46117 Liberec, Czech Republic

# Comparison of Thermal Performance of Firefighter Protective Clothing at Different Levels of Radiant Heat Flux Density

## *Primerjava učinkovitosti toplotne zaščite oblek za gasilce pri različnih stopnjah sevanja toplotnega toka*

Original Scientific Article/*Izvirni znanstveni članek*
Received/ *Prispelo* 04-2018 • Accepted/ *Sprejeto* 08-2018

## Abstract

The experimental work presented in this study is related to the investigation of thermal protective performance of firefighter clothing, which plays a pivotal role in the firefighters' safety and performance. The firefighter clothing usually consists of three layers, i.e. an outer shell, moisture barrier and thermal liner. Four samples were used for the purpose of this study. The samples were characterized on Alambeta for the evaluation of thermal resistance and thermal conductivity, respectively. Afterwards, the samples were evaluated on a thermal manikin "Maria" at room temperature to measure the insulation values. Moreover, air permeability was evaluated by using an air permeability tester. The samples were then analysed for their thermal protective behaviour in line with a slightly modified ISO standard 12127, i.e. the samples were subjected to 150 °C heat plate at constant speed. In addition, transmitted heat flux density and percentage transmission factor of all samples were determined with the help of a radiant heat flux density machine at 10 kW/m$^2$ and 20 kW/m$^2$. It was concluded that sample 4 had higher thermal resistance and insulation values. The outer shell of sample 4 had lower air permeability values as compared to the outer shell of samples 1, 2 and 3. Similarly, the combination of the outer shell 4 and the thermal barrier 4 led to lower air permeability values as compared to the combination of the outer shell 1 and thermal barrier 1, outer shell 2 and thermal barrier 2, and outer shell 3 and thermal barrier 3. The rate of temperature rise in sample 4 occurred at a slower rate against the heated plate in comparison with samples 1, 2 and 3. Furthermore, sample 4 exhibited lower transmitted heat flux density and percentage transmission factor as compared to samples 1, 2 and 3.
Keywords: multilayer protective clothing, thermal radiation, radiant heat transmission index, flame

## *Izvleček*

*Raziskava je bila osredotočena na učinkovitost toplotne zaščite oblek za gasilce, ki je ključnega pomena za varnost in učinkovito delo gasilcev. Oblačila za gasilce običajno sestavljajo tri plasti, tj. zunanja plast, paroprepustna plast in toplotnoizolacijska plast. V raziskavo so bili vključeni štirje vzorci. Z Alambeto so bile značilne lastnosti vzorcev za oceno toplotnega upora oziroma toplotne prevodnosti. Nato so bile pri sobni temperaturi določene izolacijske vrednosti na toplotni poskusni lutki »Mariji«. Ovrednotena je bila tudi zračna prepustnost vzorcev na aparatu za prepustnost zraka. Vzorci so bili nato analizirani z vidika sposobnosti toplotne zaščite s pomočjo nekoliko spremenjene standardne metode ISO 12127 z izpostavitvijo vzorcev temperaturi do 150 °C na toplotni plošči pri konstantni hitrosti. S pomočjo sevalne naprave pri toplotnih tokih 10 kW/m$^2$ in 20 kW/m$^2$ sta bila določena tudi prenos toplotnega toka ter faktor prenosa vseh vzorcev. Ugotovljeno je bilo, da ima vzorec 4 visok toplotni upor in toplotno izolativnost. Zunanja plast vzorca 4 je imela nižje vrednosti zračne prepustnosti kot zunanje plasti vzorcev 1, 2 in 3. Podobno je v primerjavi z vzorci 1, 2 in 3 imela kombinacija zunanje plasti skupaj s toplotnoizolacijsko plastjo vzorca 4 nižjo*

Corresponding author/*Korespondenčni avtor:*
**Jawad Naeem**
E-mail: jawadnaeem.qau@gmail.com

*Tekstilec, 2018,* ***61****(3), 179-191*
*DOI: 10.14502/Tekstilec2018.61.179-191*

*vrednost zračne prepustnosti. Prav tako je temperatura v vzorcu 4 na grelni plošči naraščala počasneje kot v vzorcih 1, 2 in 3. Vzorec 4 je imel tudi nižji prenos toplotnega toka in nižji faktor prenosa v primerjavi z vzorci 1, 2 in 3.*
*Ključne besede: večplastna varovalna obleka, toplotno sevanje, faktor prenosa sevane toplote, ogenj*

## 1 Introduction

Clothing not only serves as a barrier to the exterior atmosphere but also acts as a heat transmission channel from the human body to the surrounding atmosphere [1]. A microclimate is generated by the clothing between the human skin and air layer, which assists the thermoregulatory mechanism of the human body to maintain its temperature within a safe limit, despite the exterior environmental temperature and humidity deviating to some degree [2–4]. The exchange of heat in clothing includes conduction via the air gap and fabric layer, convection of the air gap and radiation from the fabric layer to another fabric layer [5]. In some situations, protection against flame and heat becomes primary precedence for a specific area of applications like firefighting, where a shield against flame and thermal insulation is required [6]. The firefighters' lives are always in continual danger when they are subjected to an escalated temperature climate, high thermal radiation, interaction with hot objects and confrontation to several types of flame, flash fire being the most dangerous [7]. The firefighter protective clothing shields the firefighter from hazards like spilling of chemicals, flame, external radiant heat flux, and offers a thermal equilibrium to their body [8]. The firefighter protective clothing consists of three layers, i.e. an exterior shell, moisture barrier and thermal liner [8–10]. The exterior shell is made up of the substrates which do not burn or degenerate when they are confronted against the heat and flame. These materials avert ignition when they are in contact with flame, and must be water repellent and permeable to water vapour. Generally, the outer shell is made up of meta-aramid (Nomex), and a combination of meta-aramid and para-aramid (Nomex III A), polybenzimidazole (PBI), Zylon. Sometimes, flame resilient finishes like Proban and Pyrovatex are employed as well. The moisture barrier is a microporous or hydrophilic membrane situated between the thermal liner and outer shell. This membrane is permeable to water vapour but impermeable to liquid water, and protects the human body from blood pathogens and chemicals in liquid form. This membrane is accessible in market as Gore-Tex, Proline and Cross tech, Action and Neo guard. The thermal liner secures the human body by delaying the external environment heat. It is made up of flame retardant fibres and their blends. They can be non-woven, laminated woven, quilted batting and spun laced [10–12]. The schematic diagram of a multilayer assembly is shown in Figure 1.

Time is the main factor when the thermal protective performance is evaluated. An escalation in the thermal protective performance (TPP) means an increment in the duration of time for firefighters to conduct their duties without enduring any severe skin burn injuries. Consequently, more time can be spent by the firefighter to save lives and prevent damages instigated by fire and heat [14–16].

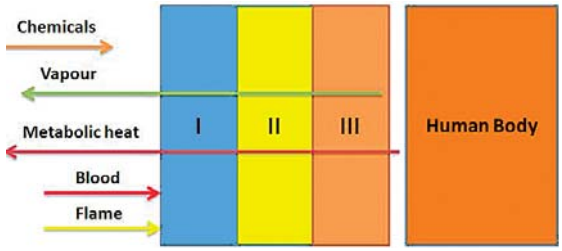


*Figure 1: Configuration of multilayer protective clothing [10, 13]*
*I – outer shell, II – moisture barrier, III – thermal liner*

Factors like thermal conductivity, water vapour resistance, volumetric flow capacity, permeability index and effect of air gaps can have an impact on the thermal protective performance of firefighters' clothing (FFC) [17]. The evaluation of TPP can be performed by several tests (heat guard plate, TPP tester) [18–22] or the full-scale testing method (thermal manikin) [23–24].

A lot of scientific research in the form of numerical models and experimental studies has been conducted under various levels of radiant heat flux density to evaluate the thermal protective performance of FFC. These studies have made use of the test methodologies like bench scale testing and full manikin test to determine the thermal protective performance of FFC under various levels of radiant heat exposure.

The aim of this study was to investigate the thermal protective performance of different FFC samples.

Four different sample arrangements were made. These samples were tested with Alambeta, thermal manikin Maria and air permeability tester FX 3300. The threshold time, $t$ (s), was measured in accordance with the ISO 12127 standard. Afterwards, these samples were characterized with a radiant heat transmission machine (ISO 6942 method) to determine the heat transmission through a sample at 10 kW/m$^2$ and 20 kW/m$^2$. Moreover, transmitted heat flux density, $Q_c$ (kW/m$^2$), percentage transmission factor, $\%TF(Q_o)$ and radiation heat transmission index ($RHTI_{12}$ and $RHTI_{24}$) were determined.

## 2 Experimental

### 2.1 Materials

All firefighter clothing (FFC) was provided by Vochoc Ltd (Czech Republic). Each clothing item consisted of three layers, i.e. outer layer, moisture barrier and thermal liner. Four different clothing items with different material combinations were used in this research. The material specifications taken from firefighter clothing items (Table 1) and their arrangement in the clothing assembly are listed below (Table 2).

*Table 1: Material specifications*

| Material code | Material specification | Material function | Weave | Mass per unit area [g/m$^2$] |
|---|---|---|---|---|
| O1 | 55% Conex, 38% Lenzing FR, 5% Twaron, 2% Beltron | Outer shell | Rip stop | 215 |
| MB1 | Fabric:100% polyester<br>TOPAZ high tech PU | Moisture barrier | Non-woven | 145 |
| TB1 | Thermo: para-aramid<br>Liner: 50% meta-aramid, 50% viscose | Thermal liner | Non-woven | 200 |
| O2 | 75% Nomex, 23% Kevlar, 2% P-140 | Outer shell | Rip stop | 195 |
| MB2 | Fabric: 50% Kermel, 50% viscose FR<br>PTFE membrane | Moisture barrier | Non-woven | 120 |
| TB2 | Thermo: para-aramid<br>Liner: 50% meta-aramid, 50% viscose | Thermal liner | Non-woven | 200 |
| O3 | 55% Conex, 38% Lenzing FR, 5% Twaron, 2% Beltron | Outer shell | Rip stop | 215 |
| MB3 | Fabric: 50% Kermel, 50% viscose FR<br>PTFE membrane | Moisture barrier | Non-woven | 120 |
| TB3 | Thermo: para-aramid<br>Liner: 50% meta-aramid, 50% viscose | Thermal liner | Non-woven | 200 |
| O4 | 70% Conex, 23% Lenzing FR, 5% Twaron, 2% Beltron | Outer shell | Rip stop | 225 |
| MB4 | Fabric: 50% Kermel, 50% viscose FR<br>PTFE membrane | Moisture barrier | Non-woven | 120 |
| TB4 | Thermo: para-aramid<br>Liner: 50% meta-aramid, 50% viscose | Thermal liner | Non-woven | 200 |

*Table 2: Sample specifications*

| Sample No. | Sample assembly | Thickness [mm] | Mass per unit area [g/m$^2$] |
|---|---|---|---|
| 1 | O1 + MB1 + TB1 | 2.636 | 560 |
| 2 | O2 + MB2 + TB2 | 2.703 | 515 |
| 3 | O3 + MB3 + TB3 | 2.759 | 535 |
| 4 | O4 + MB4 + TB4 | 2.77 | 545 |

## 2.2 Methods

### 2.2.1 Alambeta

Alambeta is a computer-controlled non-destructive device. With the help of Alambeta, the thermal properties of single layer and multilayer fabrics are determined [25–27]. It is non-destructive equipment which comprises of a movable hot plate attached to an ultrathin heat flow sensor on the top side and a lower cold plate. This upper heated plate falls in downward direction and makes a contact with the surface of the sample which is placed on the lower cold plate. The computer records the heat flow due to the differentiation in temperature between the upper heated plate and the sample on the cold plate. The temperature of the upper plate is held at 32 °C, where as the lower plate is kept at ambient temperature, i.e. at around 20 °C. With the help of Alambeta, characteristics like thermal conductivity, thermal diffusivity, thermal absorptivity, thermal resistance, sample thickness, and heat flow density and heat flow density ratio can be determined [28–29]. In this research, each sample was evaluated five times.

### 2.2.2 Thermal manikin

A thermal manikin Maria (Figure 2) was used to measure the thermal insulation values of firefighter protective clothing samples. The manikin is built up of fibre glass armed polyester shell covered with a thin nickel wire enveloped around the body to ensure the heating and temperature measurement. The design of shoulder, hip and knee joints was made of a circular cut to make the sitting and standing positions normal.

*Figure 2: Thermal manikin Maria with left forearm covered with sample of firefighter protective clothing*

During the testing, the manikin was positioned at the centre of the climatic chamber and was kept in a supporting frame, hung from the head and with the feet 0.15 m away from the floor. The manikin had 20 independent parts managed by a computer according to the association between dry heat losses and skin temperature of the human body for the conditions close to thermal comfort [29].

In our experiment, the forearm limb portion of the manikin was covered with a forearm sleeve, since the forearm limb area was much lesser as compared to the other parts of the manikin where less fabric was used.

**Global method**

The global method is a general formula for defining the whole body resistance. It is a conventional method which performs an overall calculation and defines whole body resistance. In equation1, $f_1$ is the relationship between the surface area of the segment $I$ of the manikin, $A_i$, and the total surface area of the manikin, $A$. $T_0$ is the temperature of the operating environment in degrees centigrade (°C). $\bar{T}_{sk}$ is the mean skin temperature in °C and $\bar{\dot{Q}}_{s,i}$ is the sensible heat flux acquired by area weighing (W/m²). First, the thermal insulation of a nude manikin, $I_a$, was calculated.

$$I_T = \frac{\Sigma(f_i \times \bar{T}_{sk,i}) - T_0}{\Sigma(f_i \times \bar{\dot{Q}}_{s,i})} \quad (1)$$

After subtracting $I_a$ from $I_T$, the effective clothing insulation, $I_{cle}$, (m² °C/W) was acquired.

$$I_{cle} = I_T - I_a \quad (2)$$

To calculate the intrinsic thermal insulation, $I_{cl}$ was calculated with equation 3:

$$I_{cl} = I_T - \frac{I_a}{f_{cl}} \quad (3),$$

where $f_{cl}$ is the ratio of the outer surface area of a clothed body to the surface area of a nude body.

### 2.2.3 Air permeability

An air permeability tester FX3300 Labotester III (Textest Instruments) was utilized to evaluate air permeability in line with the CSN EN ISO 9237 standard. The test pressure was 200 Pa on the area of 20 cm² (l/m²/s). Ten measurements were performed for each sample according to the standard.

### 2.2.4 Contact heat plate test

The contact heat plate test was used to characterise the thermal protective performance of firefighter protective clothing. An experimental setup was made, the basic principle was derived from slight modification of ISO standard 12127 [30].

The hot plate was heated to and maintained at constant temperature, and a thermocouple was placed on the top of a test sample. The sample was lowered down towards the heated cylinder. The operation was conducted at constant speed. The threshold time was evaluated by monitoring the temperature rise of the thermocouple.

The samples of FFC were cut to 15 cm diameter and then attached on to a ring shape frame. The latter was made fixed on a circular clamp with the help of a magnet and thermocouple on the top and middle of a sample. The clamp was attached to a dynamometer. The heated plate (heat source) was maintained at constant temperature of 150 °C, as the firefighter protective fabric test samples were made up of meta-aramids, which has maximum continuous temperature usage at 150 °C. A schematic diagram is shown in Figure 3. The samples were raised to the height of 60 mm above the heated plate with the help of a dynamometer and afterwards brought down towards the heated plate. When the distance between the heat plate and the sample was 10mm, we recorded the time and noted the temperature of the sample until there was a 10 °C rise in temperature. Afterwards, we removed the heat source away from the sample and allowed the thermocouple and clamps to cool down for the next sample to be evaluated. The samples were brought towards the heated plate at the constant speed of 5mm/min [30]. The test procedure had to be performed on three samples to get the average value. The arrangement of the contact heat test is depicted in Figure 4.

The apparatus consists of a heat plate, digital multimeter, T type thermocouple, clamps and a dynamometer:

- Heat plate which is VWR® professional hot plate developed for applications requiring exceptional accuracy, stability, and repeatability are equipped with an exclusive safety system that helps protect both the operator and sample.
- Digital multimeter Velleman DVM 345DI was employed to evaluate the temperature changes in the sample. This device enables the user to measure AC and DC voltages, AC and DC currents, resistance, capacitance and temperature. The device can be interfaced with a computer and the user can also test diodes, transistors and audible continuity.
- T type thermocouple "UT-T" with the temperature probe test range from –40 to +260 °C with the accuracy of ±0.75% was utilized. Circular clamps were employed to hold the sample.
- Dynamometer was used to move the test sample at the constant speed of 5 mm/min from fixed distance.

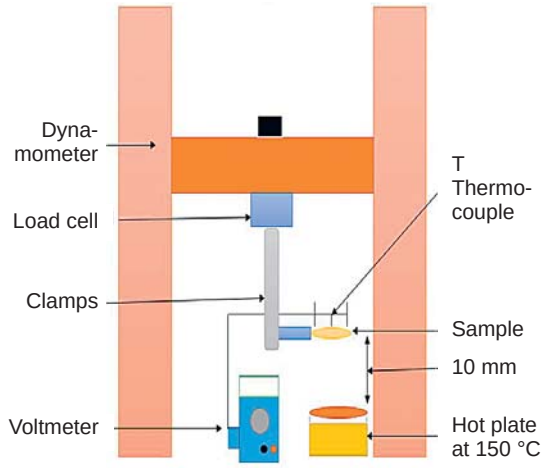


*Figure 3: Schematic diagram of contact heat test arrangement*

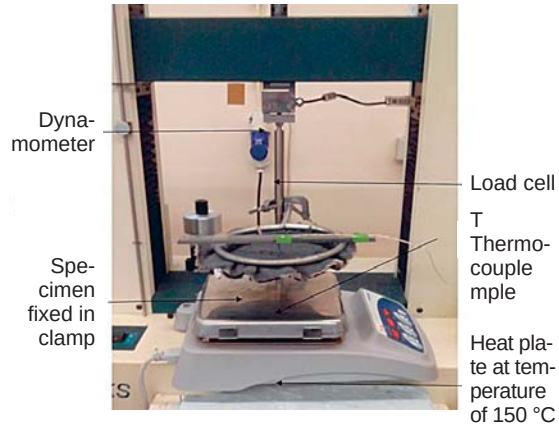


*Figure 4: Arrangement of contact heat test*

### 2.2.5 Transmission of radiant heat flux density

The equipment consists of a radiation heat source, which can generate heat flux density of up to 80 kW/m$^2$ along with a calorimeter to determine the radiant heat flux density.

The ISO 6942 standard was employed to measure the transportation of heat through a single layer and

multilayer FFC sample. The sample dimension was 230 mm × 80 mm. All samples had to be conditioned for at least 24 hours at the temperature of 20±2 °C and had relative humidity of 65±2% [31].
The apparatus included a curved copper plate calorimeter placed on a non-combustible block. The front face of the calorimeter was layered with a thin film of black paint with the absorption coefficient "a" greater than 0.9. The heating device comprised of six carbide rods, a moving frame assembly which was constantly cooled by a passage of water in cooling pipes and a removable screen. The first step started with calibration, the position of the calorimeter was adjusted and then the calorimeter was exposed to the heating rods and the movable screen was withdrawn and returned to its original position when the temperature escalation reached 30 °C. The incident heat flux density, $Q_0$, was measured. Later on, the sample was affixed to one side of the plate of the sample holder and held in contact with the face of the calorimeter, applying the mass of 200 g. The movable screen was withdrawn and the starting point of the radiation head was noted. The movable screen was returned to its closed position after the temperature rise of about 30 °C. The time $t_{12}$was to achieve the temperature rise of 12.0±0.1 °C and the time$t_{24}$ to achieve the temperature rise of 24±0.2 °C in the calorimeter, expressed in seconds, determined to the nearest 0.1 s. At least three samples had to be tested to get the average value [31]. Figure 5 shows the arrangement of the radiant heat testing equipment.

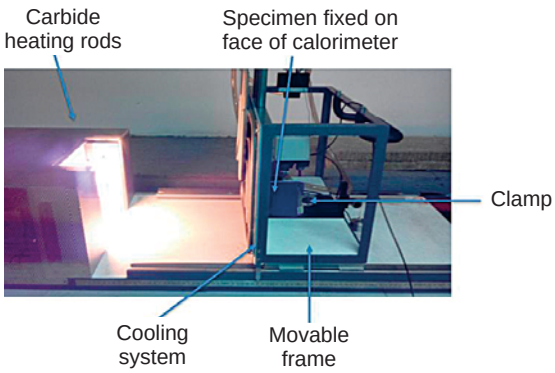


*Figure 5: Radiation heat testing equipment*

The conclusion of the experimentation led to two threshold times, i.e. radiant heat transfer index ($RHTI_{12}$ and $RHTI_{24}$), transmitted heat flux density ($Q_c$) and percentage heat transmission factor $\%TF(Q_o)$

The transmitted heat flux density, $Q_c$, in kW/m$^2$ was calculated with the following equation:

$$Q_c = \frac{MC_p}{A} \times K \quad (4),$$

where M (kg) is the mass of the copper plate, $C_p$ is the specific heat of copper 0.385 kJ/kg°C, $A$(m$^2$) is the area of the copper plate, K (°C/s) is the mean rate of temperature rise in the calorimeter in the region12–24 °C rise.

$$K = \frac{12}{RHTI_{24} - RHTI_{12}} \quad (5),$$

where $RHTI_{12}$ indicates the time (s) required for the temperature rise of 12±0.1 °C, and $RHTI_{24}$ means the time for the temperature rise of 24±0.2 °C in the calorimeter.
The percentage heat transmission factor, $\%TF(Q_o)$, for the incident heat flux density level was determined with equation 6.

$$\%TF(Q_0) = \frac{Q_c}{Q_0} \times 100 \quad (6),$$

where $Q_0$ is the incident heat flux density (equation 7).

$$Q_0 = \frac{C_p RM}{a \cdot A} \quad (7),$$

where $R$ (°C/s) is the rate of the calorimeter temperature rise in the linear region and $a$ is the absorption coefficient of the painted surface of calorimeter.

## 3 Results and discussion

### 3.1 Evaluation of thermal properties

The thermal insulation of protective clothing plays a very important role in the thermal protective performance of firefighter protective clothing. The main purpose of fire fighter protective clothing is to delay the increase in temperature of the human body when they are exposed to a heat source and consequently to enhance the firefighters' working time when saving lives and valuables. The ability of a textile substrate to conduct heat is called thermal conductivity of a textile material. A greater value of thermal conductivity indicates a greater amount of heat exchange passing through that substrate. However, the thermal conductivity of a textile substrate is determined by the physical and chemical properties of the textile substrate [32]. An increment in the relative humidity absorbed by the substrate is followed by an increase in the thermal conductivity of the textile substrate

[34]. Consequently, the more a material is hygroscopic, the better is thermal conductivity. Thermal resistance is associated with thickness, surface weight and density. For thickness, it can be explained that at equivalent surface weights, increasing the thickness leads to an increase in the amount of air entrapped in the fabric. This is confirmed by the fact that thermal resistance decreases by increasing density as higher density means less air entrapped in the textile. In consequence, a thick fabric has higher thermal resistance as compared to a light and thin textile substrate [33]. This is also described by the mathematical formula: $R = h/\lambda$, where $R$ is thermal resistance, $h$ is thickness and $\lambda$ thermal conductivity. Moreover, it is influenced by the fabric construction parameters. Thus, a thick and heavy fabric is more insulative than a thin and light one [35]. Table 1 reveals that sample 4 had slightly greater thickness than other samples, which might be one reason for better thermal insulation and increased thermal resistance as compared to other samples. As the thickness of sample 1 was smaller than the rest of samples, sample 1 had significantly lower values of thermal resistance and total thermal insulation, and clo values as compared to the rest of samples. This was also evident by the ANOVA test as the $p$-value was $7.35\times10^{-5}$, i.e. less than 0.05, indicating a significant difference among the samples. Furthermore, the constituent material of the substrate plays a very important role in the thermal insulation/thermal resistance of firefighter protective clothing [36]. The results of Alambeta in Figure 6 also support the outcomes (insulation and clo values) in Figures 7 and 8 for the thermal manikin, i.e. greater thermal insulation, which results in lower thermal conductivity and enhanced thermal resistance.

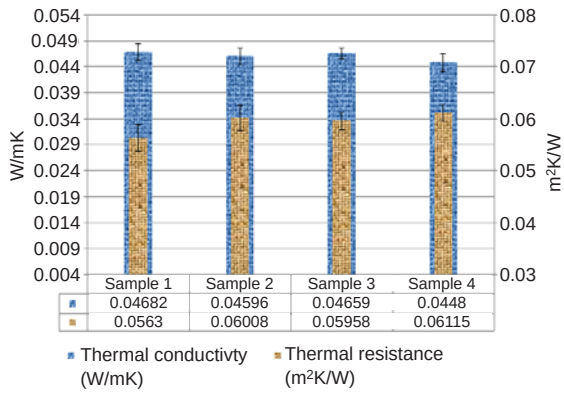


*Figure 6: Analysis of thermal characteristics with Alambeta*

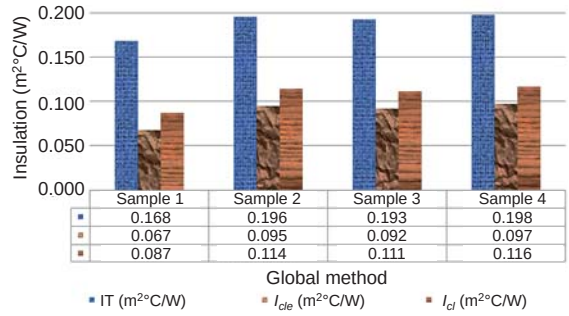


*Figure 7: Total thermal insulation ($I_T$), effective clothing insulation ($I_{cle}$) and basic insulation ($I_{cl}$) of firefighter protective sample*

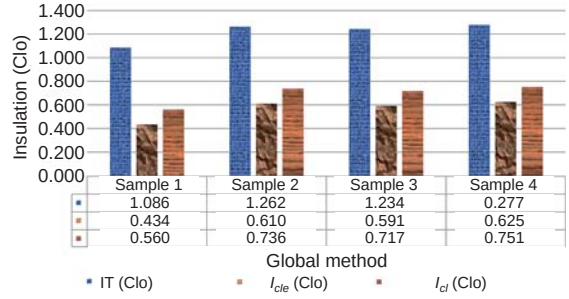


*Figure 8: Total clothing insulation ($I_T$), effective clothing insulation ($I_{cle}$) and basic clothing insulation ($I_{cl}$) in clo*

## 3.2 Evaluation of air permeability

As the air permeability of the moisture barrier in firefighter protective clothing is zero, the evaluation of the air permeability of the outer shell and outer shell + thermal barrier was conducted. The air permeability of firefighter protective clothing is very low, since the main task of firefighter protective clothing is to protect the firefighter's body from the heat in the form of radiation, convection and conduction. If the value of air permeability is very high, it decreases the thermal protective performance of firefighter clothing as it allows the air to pass through the sample resulting in the temperature increase of the human body within a shorter period of time. It can be seen in Figure 9 that the outer shell of sample 4 exhibited lower air permeability values as compared to the outer shell of samples 1, 2 and 3. Figure 10 shows that sample 4 had a lower value of air permeability as compared to the rest of samples in the case of the outer shell and outer shell + thermal barrier, and this low value is supported by the high value of thermal insulation and low values of thermal conductivity as evaluated by the thermal manikin and Alambeta, respectively.

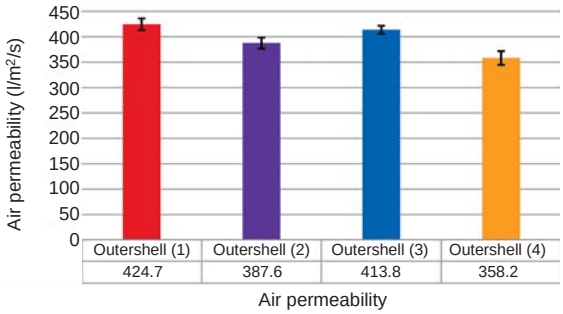


*Figure 9: Air permeability of outer shell of firefighter protective samples*

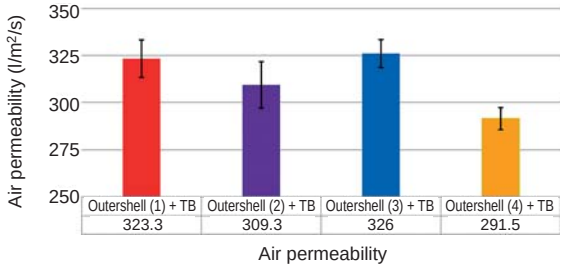


*Figure 10: Air permeability of outer shell + thermal barrier of firefighter protective clothing*

## 3.3 Contact heat plate test at 5mm/min exposing speed

In Table 3 and Figure 11, it can be seen that sample 4 took more time for the increment of 10 °C rise in temperature when exposed to the heat source (150 °C) at the constant speed of 5 mm/min. Furthermore, when the sample was at 10 mm distance from the heat source, the temperature at the back of sample 4 was lower as compared to other samples at the same distance. There are two possible reasons for better thermal protective performance of the clothing. One is the thickness and the other is the physical and chemical properties of constituent fibres in the fabric. In the case of sample 4, thickness was slightly higher as compared to the rest of samples; the sample had a higher percentage of meta-aramid in the outer shell, enhancing the thermal protective performance and delaying the rate of the temperature rise.

The greater the delay in the heat transmission towards the human body, the greater is the thermal protective performance of the clothing, enabling the firefighters to spend more time on duty.

*Table 3: Threshold time in contact heat test at exposing speed of 5mm/min*

| Sample No. | $T_c$ [°C] | $T_1$ [°C] | $T_2$ [°C] | $t$ [s] |
|---|---|---|---|---|
| 1 | 150 | 49±1 | 60.3±1.53 | 91 |
| 2 | 150 | 44.3±1.15 | 54.7±0.58 | 106 |
| 3 | 150 | 46.7±1.53 | 58.3±1.53 | 101 |
| 4 | 150 | 41.7±0.58 | 52.7±1.15 | 111 |

$T_c$ – contact temperature of hot plate
$T_1$ – initial temperature at the back of sample when at the distance of 10 mm from hot plate
$T_2$ – final temperature at the back of a sample when there is a 10 °C rise in temperature
$t$ – threshold time for increase of 10 °C

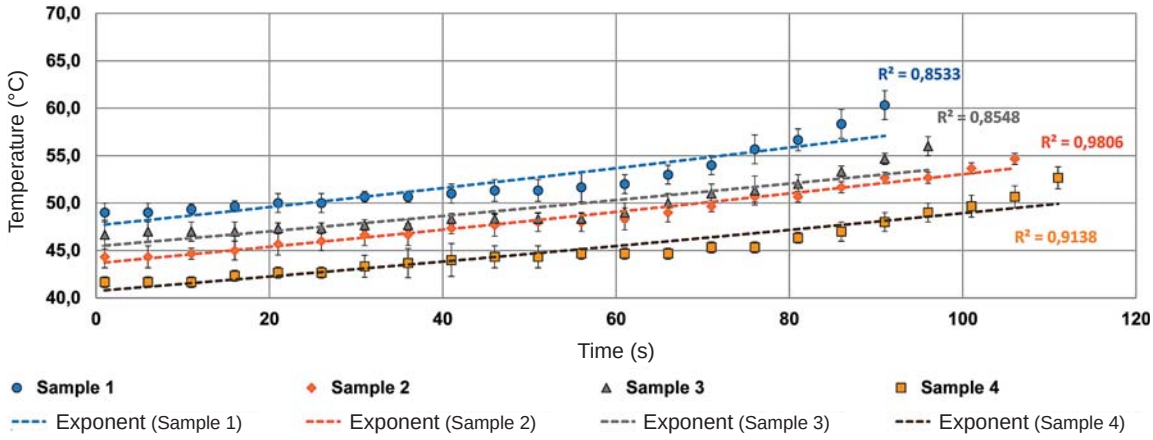


*Figure 11: Contact temperature and thermal protective performance of firefighter clothing at exposing speed of 5 mm/min*

### 3.4 Transmission of radiant heat flux through multilayer protective clothing

A generic overview of Table 4 reveals that with the increase in the value of the incident heat flux density from 10 kW/m$^2$ to 20 kW/m$^2$, the values of transmitted heat flux density, $Q_c$, (kW/m$^2$) and percentage transmission factor $\%TF(Q_o)$ increase successively at all samples. On the other hand, a reverse trend was observed for the values of the radiant heat transmission index $RHTI_{24} - RHTI_{12}$ (s). The smaller the values of transmitted heat flux density, the lesser the amount of heat flowing through the FFC sample towards the calorimeter. In consequence, firefighters are able to continue with their activities for a lengthier period before acquiring skin burn injuries. Table 4 also illustrates that a greater difference between $RHTI_{24}$ (s) and $RHTI_{12}$ (s) shows that the sample is able to withstand the respected incident heat flux density for a longer duration before having burn wounds.

At $Q_o$ of 10 kW/m$^2$, samples 1 and 3 depicted higher values of $Q_c$ (kW/m$^2$) as compared to samples 2 and 4, respectively. $Q_c$ (kW/m$^2$) values of samples 1 and 3 were very close to each other. A slightly different pattern was witnessed for FFC samples at $Q_o$ of 20 kW/m$^2$. Sample 1 depicted very high values of $Q_c$ and $\%TF(Q_o)$ as compared to all samples. Samples 2 and 3 exhibited very close values of $Q_c$ and $\%TF(Q_o)$. However, the lowest value of $Q_c$ and $\%TF(Q_o)$ was witnessed at sample 4.

Sample 1 had relatively smaller thickness as compared to all other samples due to which it delivered higher values of $Q_c$ and $\%TF(Q_o)$ at both 10 kW/m$^2$ and 20 kW/m$^2$. In the case of sample 2, it had slightly smaller thickness as compared to samples 3 and 4. Nevertheless, it had a lower value of $Q_c$ and $\%TF(Q_o)$ as compared to sample 3. This might be due to the fact that sample 2 had higher percentage of meta-aramid in the outer shell, assisting the endurance against radiant heat flux density for a longer period of time, and delivered lower values of $Q_c$ and $\%TF(Q_o)$.

Sample 4 had slightly higher thickness and greater percentage of meta-aramid in the outer shell as compared to the rest of samples due to which the transmission of heat was delayed, and smaller values of $Q_c$ and $\%\ TF(Q_o)$ were observed at both 10 kW/m$^2$ and 20 kW/m$^2$.

At $Q_o$ of 10 kW/m$^2$, samples 1 and 3 depicted higher values of $Q_c$ (kW/m$^2$) as compared to samples 2 and 4, respectively. The $Q_c$ (kW/m$^2$) values of samples 1 and 3 were very close to each other. A slightly different pattern was witnessed for the FFC samples at $Q_o$ of 20 kW/m$^2$. Sample1 depicted very high values of $Q_c$ and $\%TF(Q_o)$ as compared to all the samples. Samples 2 and 3 exhibited very close values of $Q_c$ and $\%TF(Q_o)$. However, the lowest value of $Q_c$ and $\%TF(Q_o)$ was witnessed at sample 4.

Sample 1 had relatively smaller thickness as compared to all other samples due to which it delivered higher values of $Q_c$ and $\%\ TF(Q_o)$ at both 10 kW/m$^2$ and 20 kW/m$^2$. Sample 2 had slightly smaller thickness as compared to samples 3 and 4. Never the less, it had a lower value of $Q_c$ and $\%TF(Q_o)$ as compared to sample 3. This might be a consequence of sample 2 having greater percentage of meta-aramid in the outer shell, assisting the endurance against radiant heat flux density for a longer period of time, and delivering a lower value of $Q_c$ and $\%TF(Q_o)$.

*Table 4: Comparison of transmitted heat flux density and incident heat flux density at 10 and 20 kW/m²*

| Sample No. | $Q_o$ [kW/m$^2$] | $RHTI_{12}$ [s] | $RHTI_{24}$ [s] | $RHTI_{24} - RHTI_{12}$ [s] | $Q_c$ [kW/m$^2$] | $TF\ (Q_o)$ [%] |
|---|---|---|---|---|---|---|
| 1 | 10 | 34.35±0.919 | 53.9±0.697 | 19.55 | 3.382 | 33.8 |
| 2 | | 37.4±0.282 | 61±0.424 | 23.6 | 2.8022 | 28.0 |
| 3 | | 37.6±1.181 | 59.4±1.939 | 21.8 | 3.033 | 30.3 |
| 4 | | 44.25±0.495 | 72.9±0.848 | 28.65 | 2.308 | 23.0 |
| 1 | 20 | 21.95±0.070 | 31.35±0.141 | 9.4 | 7.035 | 35.1 |
| 2 | | 25.9±0.282 | 38.65±0.353 | 12.75 | 5.1868 | 25.9 |
| 3 | | 26.7±1.979 | 38.35±1.757 | 11.65 | 5.676 | 28.3 |
| 4 | | 28.95±0.474 | 43.3±0.676 | 14.35 | 4.608 | 23.0 |

Sample 4 had slightly greater thickness and higher percentage of meta-aramid in the outer shell as compared to other samples, due to which the transmission of heat was delayed and lower values of $Q_c$ and % *TF* ($Q_o$) were observed at both 10 kW/m$^2$and 20 kW/m$^2$.

Figure 12 shows that in the first 12 seconds, the rate of temperature rise in all samples was almost equal. However, afterwards, the rate of temperature rise of sample 4 occurred at a much slower rate; therefore, a flatter curve was seen. In the case of sample1, a steeper curve was observed, which indicated that the rate of temperature rise was greater as compared to the rest of samples. For samples 2 and 3, the curve pattern was very similar until the 35$^{th}$ second. Afterwards, the curve of sample 2 became slightly flatter as compared to the curve of sample 3, indicating a slightly better thermal protective performance of sample 2 as compared to sample 3. The flatter the curve, the more time was required to rise the

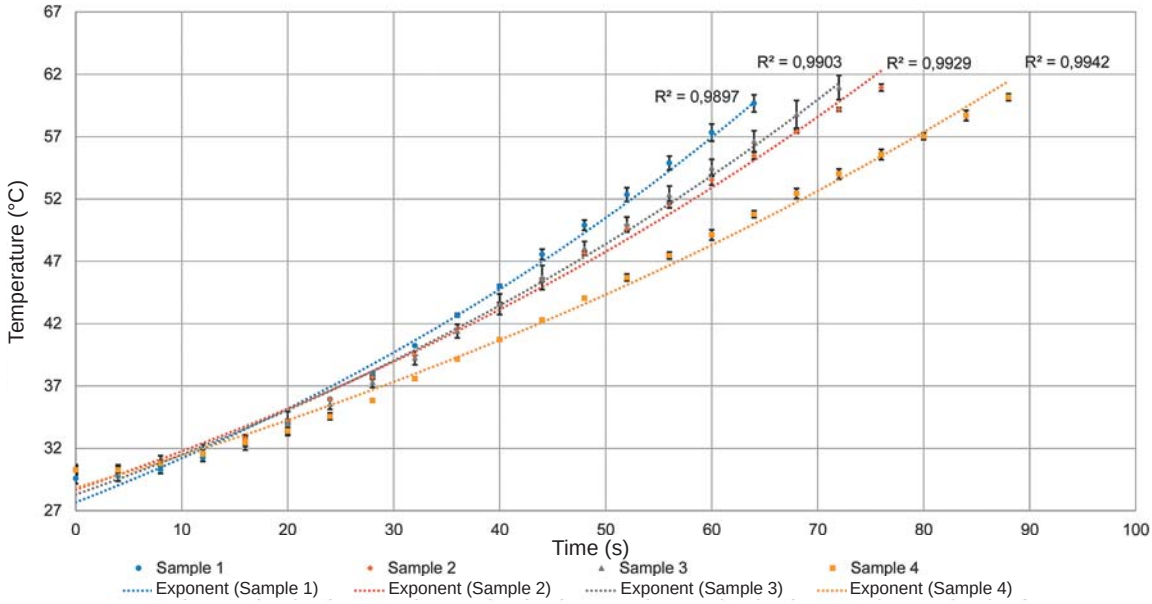


*Figure 12: Transmission of heat through FFC sample at 10 kW/m$^2$*

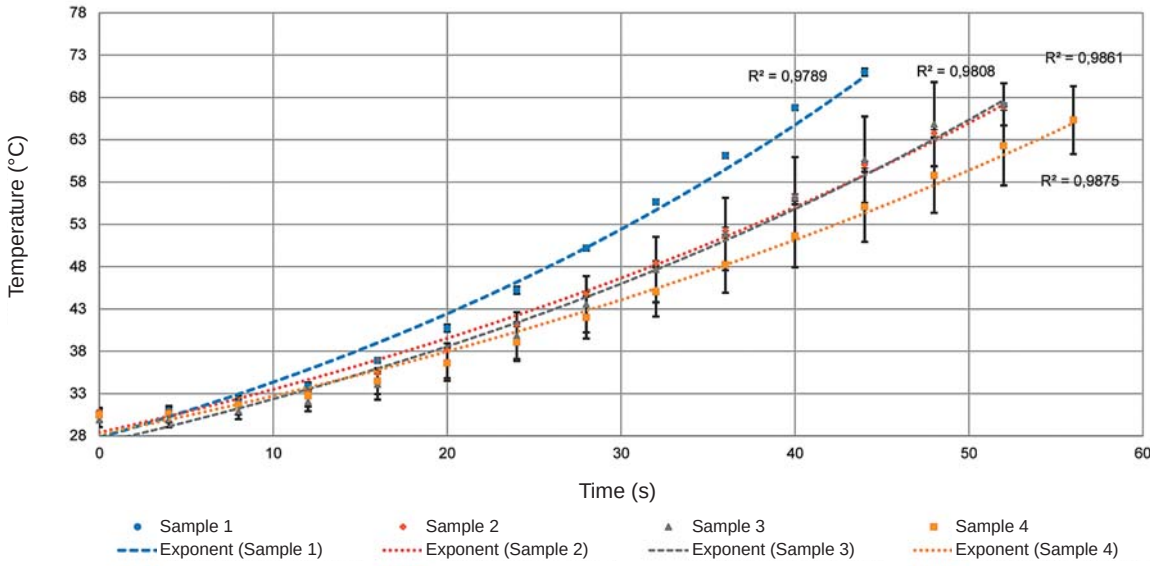


*Figure 13: Transmission of heat through FFC samples at 20 kW/m$^2$*

temperature on the other side adjacent to the calorimeter, due to which the amount of heat was delayed and lower values of $Q_c$ (kW/m$^2$) and $\%TF(Q_o)$ were noted by the calorimeter. As a result, firefighters are able to endure the heat for a longer period of time and perform their activities before acquiring any harmful injuries.

At 20 kW/m$^2$, the curve pattern of samples 4 and 1 was similar to that of the curves for 10 kW/m$^2$. However, this time, the curve of sample 3 was flatter as compared to the curve of sample 2 and both curves were overlapping each other from the time of 40–57 seconds. Afterwards, the curve of sample 2 was slightly flatter than the curve of sample3. It was also noticed that in Table 4, at 20 kW/m$^2$, the value of $Q_c$ relatively increased for each sample as compared to the value of $Q_c$ for 10 kW/m$^2$ due to which steeper curves were acquired indicating the rate of temperature rise occurring at a faster rate.

## 4 Conclusion

The firefighters's safety is influenced by the protective performance of firefighter protective clothing. If the thermal protective behaviour of FFC can succeed in enhancing the confrontation time of firefighters against radiant heat flux density, they will be able to save more lives and assets. The research showed that sample 4, which had a higher thickness value and high percentage of meta-aramid in the outer shell, displayed better thermal resistance and insulation properties as compared to the rest of samples.

The outer shell of sample 4 depicted a lower value of air permeability and the combination of outer shell + thermal barrier of sample 4 exhibited lower air permeability values values with respect to other samples. Furthermore, the time of exposure to the heat plate at the constant temperature of 150 °C was longer in the case of sample 4. All these results suggest that sample 4 had slightly better thermal properties as compared to the rest of samples.

Sample 4 yielded lower values of *Qc* and $\%TF(Q_o)$ in comparison to all other samples. However, with the increase in the level of incident flux density, there was also enhancement in the values of $Q_c$ and percentage transmission values for all samples.

A further study is required where thermal barriers would be replaced with suitable insulating materials to determine the thermal protective performance. Additionally, the outer shell should be coated with nano-metallic particles like silver, $Al_2O_3$ and $TiO_2$ to evaluate the thermal protective performance of FFC.

*Acknowledgments*

*This project is funded by the Technical University of Liberec, Department of Clothing Technology under SGS-2018, project reference number 21246.*

## References

1. HOLMER, Ingvar. How is performance in the heat affected by clothing? In *Textile Bioengineering and Informatics Symposium : Proceedings*. Honk Kong Polytechnic University, 2008, **1**(1), 700–705.
2. DAS, Apurba, ALAGIRUSAMY, R. Introduction to clothing comfort. In *Science in clothing comfort*. Edited by A. Das and R. Alagirusamy. Wood Head Publishing India, 2010, 1–12.
3. *Improving comfort in clothing*. Edited by G. Song. UK : Wood Head Publishing, 2011.
4. *Clothing: Comfort and Functions*. Edited by L. Fourt and N. R. S. Hollies. New York : Marcel Decker, 1970.
5. HAVENITH, George, HOLMER, Ingvar, PARSONS, Ken. Personal factors in thermal comfort assessment: clothing properties and metabolic heat production. *Energy and Buildings*, 2002, **34**(6), 581–591, doi: 10.1016/S0378-7788(02)00008-7.
6. SHAHID, Abu, FURGUSSON, Mac, WANG, Lijing. Thermophysiological comfort analysis of aerogel nanoparticle incorporated fabric for fire fighter's protective clothing. *Chemical and Materials Engineering*, 2014, **2**(2), 37–43, doi: 10.13189/cme. 2014. 020203.
7. KEISER, Corinne, ROSSI, Rene M. Temperature analysis for the prediction of steam formation and transfer in multilayer thermal protective clothing at low level thermal radiation. *Textile Research Journal*, 2008, **78**, 1025–1035, doi: 10.1177/0040517508090484.
8. LAWSON, James Randall. Fire fighters protective clothing and thermal environments of structural fire- fighting. *ASTM Special Technical Publication*, 1997, **1273**, 334–335, doi: 10.1520/STP19915S.

9. NAYAK, Rajkishore, HOUSHYAR, Shadi, PADHYE, Rajiv. Recent trends and future scope in the protection and comfort of fire-fighters' personal protective clothing. *Fire Science Reviews*, 2014, **3**(4), 1–19, doi. org/10. 1186/s40038-014-004-0.
10. JIN, Lu, HONG, Kyounga, YOON, Keejong. Effect of aerogel on thermal protective performance of firefighter clothing. *Journal of Fiber Bioengineering and Informatics,* 2013, **6**, 315–324, doi: 10.3993/jfbi09201309.
11. SONG, Guowen, PASKALUK, Stephen, SATI, Rohit, CROWN, Elizabeth M, DALE, J. Doug, ACKERMAN, Mark. Thermal protective performance of protective clothing used for low radiant heat protection. *Textile Research Journal*, 2011, **81**(3), 311–323, doi: 10. 1177/0040517510380108.
12. SCOTT, Richard A. *Textiles for protection*. UK : Woodhead publishing, 2005, 622–647.
13. JINA, Lu, HONGA, Kyoung A., NAMB, Hyun Do, YOONA, Kee Jong. Effect of thermal barrier on thermal protective performance of firefighter garments. *Journal of Fiber Bioengineering & Informatics*, 2011, **4**(3), 245–252, doi: 10.3993/jfbi09201104.
14. NEGAWO, Tolera Aderie. *Analyzing and modelling of comfort and protection properties of fire fighters protective clothings : Master thesis*. Department of Textile Engineering, Istanbul Technical University, 2015.
15. HOLCOMBE, Barry V. The heat related properties of protective clothing fabrics. *Fire safety Journal*, 1983, **6**(2), 129–141, doi: 10.1520/STP17326S.
16. ANON. *NFPA* 1971: Standard on *protective clothing ensemble* for *structural fire fighting*. *National Fire Protection Association*, *Quincy*, *MA*, *1996*.
17. SCHACHER, D., ADOLPHEAND, C., DREAN, Y. Comparison between thermal insulation and thermal properties of classical and microfibres polyester fabrics. *International Journal of Clothing Science and Technology*, 2000, 12(2), 84–95, doi: 10. 1108/09556220010371711.
18. SALMON, David. Thermal conductivity of insulations using guarded hot plates, including recent developments and sources of reference materials. *Measurement Science and Technology*, 2001, **12**(12), 1–89, doi: 10.1088/0957-0233/12/12/201.
19. HUANG, Jianhua. Thermal parameters for assessing thermal properties of clothing. *Journal of Thermal Biology*, 2006, **31**(6), 61–466, doi: 10.1016/j. jtherbio.2006.03.001.
20. ISO 11092. Textiles – Physiological Effects – Measurement of Thermal and Water Vapour Resistance Under Steady-State Conditions (Sweating Guarded Hotplate Test). *International Organization for Standardization*, 1993.
21. ASTM 1868. Standard Test Method for Thermal and Evaporative Resistance of Clothing Materials Using a Sweating Hot Plate. *American Society for Testing and Materials*, West Conshohocken, PA, 2005.
22. CHEN, Y. S., FAN, J. T., ZHANG, W. Clothing thermal insulation during sweating. *Textile Research Journal*, 2003, **73**(2), 152–157, doi: 10. 1177/004051750307300210.
23. CELCAR, Damjana, MEINANDER, Harriet, GERŠAK, Jelka. Heat and moisture transmission properties of clothing systems evaluated by using a sweating thermal manikin under different environmental conditions. *International Journal of Clothing Science and Technology,* 2008, **20**(4), 240–252, doi: 10.1108/09556220810878865.
24. LEE, Joo Young, KOEUN, Sook, LEE, Hyo Hyun, KIM, Jae Young, CHOI, Jeong Wha. Validation of clothing insulation estimated by global and serial methods. *International Journal of Clothing Science and Technology*, 2001, **23**(2/3), 184–198, doi: 10.1108/09556221111107360.
25. MATUSIAK, Malgorzata. Thermal insulation properties of single and multilayer textiles. *Fibres & Textiles in Eastern Europe*, 2006, *98–112*.
26. MATUSIAK, Malgorzata, SIKORSKI, Krzysztof. Influence of the structure of woven fabrics on their thermal insulation properties. *Fibres & Textiles in Eastern Europe*, 2011, **88**(5), 46–53.
27. HES, Lubos, ARAUJO, Mario De, DJULAY, Valentin V. Effect of mutual bonding of textile layers on thermal insulation and thermal contact properties of fabric assemblies. *Textile Research Journal*, 1996, **66**(4), 245–250, doi: 10.1177/004051759606600410.
28. MATUSIAK, Malgorzata, KOWALCZYK, Sylwia. Thermal-insulation properties of multilayer textile packages. *AUTEX Research Journal*, 2014, **14**(4), 299–307, doi: 10. 2478/aut-2014-0030.

29. OLIVEIRA, A. Virgilio, GASPAR, Adélio R., QUINTELA, Divo A. Measurement of clothing insulation with a thermal manikin operating under the thermal comfort regulation mode: comparative analysis of the calculation methods. *European Journal of Applied Physiology*, 2008, **104**(4), 679–688, doi: 10.1007/s00421-008-0824-5.
30. *ISO 12127-1. Clothing for protection against heat and flame - Determination of contact heat transmission through protective clothing or constituent materials - Part 1: Test method using contact heat produced by heating cylinder, International Organization for Standardization*, 2007.
31. MEB, Georg Wazau. GMBH Prüfsysteme. *Combustion behavior Test equipment according to ISO 6942*, 2002, Keplerstraße Berlin, 1–9.
32. SURDU, Lilioara, GHITULEASA, Carmen, MIHAI, Carmen, CIOARA, Loan. Comfort properties of multilayer textile materials for clothing. *Industria Textila*, 2013, **64**(2), 75–79.
33. OĞLAKCIOĞLU, Nida, MARMARALI, Arzu. Thermal comfort properties of some knitted structures. *Fibres & Textiles in Eastern Europe*, 2007, **15**(5–6), 64–65.
34. HES, Lubos, LOGHIN, Carmen. Heat, moisture and air transfer properties of selected woven fabrics in wet state. *Journal of Fiber Bioengineering and Informatics*, 2009, **2**(3), 141–149, doi: 10.3993/jfbi12200901.
35. VENKATARAMAN, Mohanapriya, MISHRA, Rajesh, KOTRESH, T. M., SAKOI, Tomonori, MILITKY, Jiri. Effect of compressibility on heat transport phenomena in aerogel-treated nonwoven fabrics. *The Journal of Textile Institute*, 2015, **107**(9), 1150–1158, doi: 10. 1080/00405000. 2015.1097084.
36. BARKER, Roger L., HENIFORD, Ryan C. Factors affecting the thermal insulation and abrasion resistance of heat resistant hydro-entangled nonwoven batting materials for use in firefighter turnout suit thermal liner systems. *Journal of Engineered Fibers and Fabrics*, 2011, **6**(1), 1–10.